Chemical Science

ROYAL SOCIETY OF CHEMISTRY

EDGE ARTICLE

View Article Online
View Journal | View Issue

Cite this: *Chem. Sci.*, 2025, **16**, 649

All publication charges for this article have been paid for by the Royal Society of Chemistry

In search of herbistasis: COT-metsulfuron methyl displays rare herbistatic properties†

Hui Xing,‡[a] Sarah K. M. McGregor, ‡[a] Bruna D. Batista,[ab] Cassidy Whitefield,[a] Isobella S. J. Stone,[a] Cody-Ellen Murray,[c] Rebecca M. Hurst,[c] Yizhou Liu, [a] Sharon Chow, [a] Tyler Fahrenhorst-Jones, [a] Qi Zhao, [a] Sevan D. Houston,[a] Shu-Hong Hu,[a] Thierry Lonhienne,[a] Amanda Nouwens,[a] Jed M. Burns, [a] G. Paul Savage, [d] Gimme H. Walter, [c] Luke W. Guddat, [a] Michelle A. Rafter [b] and Craig M. Williams *[a]

Received 11th October 2024
Accepted 23rd November 2024

DOI: 10.1039/d4sc06923d

rsc.li/chemical-science

Weed management is an essential intervention for maintaining food security and protecting biodiversity but is heavily reliant on chemical control measures (*i.e.*, herbicides). Concerningly, only one herbicide has been developed with a new mode of action (MOA) since the 1980s. Therefore, alternative strategies for preventing weed growth need to be explored. The lesser-known concept of halting weed growth through herbistasis could be one strategy to alleviate the lack of success in obtaining new MOA leads, but this type of activity has rarely been investigated. Herein reported is a bioisosteric cyclooctatetraene (COT) for phenyl ring replacement tactic, using the commercial acetolactate synthase (ALS) inhibitor metsulfuron methyl, that has unearthed a rare agent displaying herbistatic properties against the weed, *Cryptostegia grandiflora* (rubber vine).

Introduction

Herbicides perform an integral role in the control and management of agricultural and environmental weeds,[1,2] with their use steadily increasing each year.[3] Several hundred herbicides are commercially available and each acts in one of about 25 known modes of action (MOA).[1,2] These mostly inhibit a key protein and thus prevent plant (*i.e.* weed) growth.[4] However, herbicide resistance has developed for nearly all MOAs,[5,6] a situation described as a "wicked" problem for global food security.[7] Although dedicated research attempts to discover new MOAs to address the existing herbicide resistance problem are on-going, it has proven to be a daunting task as only one herbicide with a new MOA has been developed in the last 40 years.[8–11]

The term "herbistatic agent" was initially introduced in 1948 in the context of the herbicide, 2,4-D (**1**),[12] associating it with its synthetic auxin herbicidal activity. However, this term has garnered only sporadic mention since that time, with only three additional examples of herbistatic agents identified: (1) glaucarubolone (**2**) in 1996 – a naturally occurring quassinoid which was found to inhibit NADH oxidation in soybean cells,[13] (2) diflufenzopyr (**3**) in 1999 – assumed to block the polar transport of naturally occurring auxin indole-3-acetic acid (IAA) (**4**),[14] and

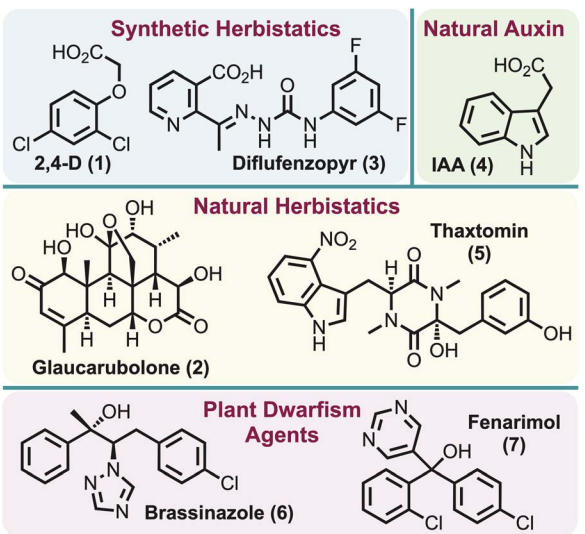

Fig. 1 Plant growth inhibitors that encompass herbistatic and plant dwarfism agents.

[a]*School of Chemistry and Molecular Biosciences, University of Queensland, Brisbane, 4072, Queensland, Australia. E-mail: c.williams3@uq.edu.au*

[b]*Health and Biosecurity, CSIRO, Ecosciences Precinct, Brisbane, 4102, Queensland, Australia*

[c]*School of the Environment, University of Queensland, Brisbane, 4072, Queensland, Australia*

[d]*CSIRO Manufacturing, Ian Wark Laboratory, Melbourne, 3168, Victoria, Australia*

† Electronic supplementary information (ESI) available: Experimental procedures, copies of NMR spectra. See DOI: https://doi.org/10.1039/d4sc06923d

‡ Joint first authors.

(3) thaxtomin (**5**) in 2013 – a bacterial phytotoxin presumed to inhibit cellulose biosynthesis[15] (Fig. 1). However, parallels can be drawn to the related "plant dwarfism" effect, where application of brassinazole (**6**),[16] or related systems such as fenarimol (**7**)[17] (Fig. 1), can induce the inhibition of the brassinosteroid biosynthetic pathway. Notably, the effects of brassinosteroid inhibition are reported to be reversible. The only identifiable definition for "herbistatic" is reported as "inhibiting the growth of weeds, which can be reversible under certain conditions".[15] This seemingly implies that both inhibition of the target enzyme and stunted plant growth are key features of herbistasis. This definition is closely analogous to that used for fungistatics (*e.g.*, azoles and echinocandins), which "halt the growth of, but does not kill the fungus"[18] and for bacteriostatics (*e.g.*, chloramphenicol, ethambutol, tetracycline).[19]

Conceptually, from a weed control perspective, treatment with a herbistatic also provides a beneficial growth advantage to agricultural or native species (*e.g.*, increased availability of essential nutrients through stunted weed growth), but a herbistatic would likely require a different mode of resistance development as the weed "killing" mechanism is absent (*i.e.* possibly extending the utility of known MOAs). The latter might be beneficial for prolonging resistance or treating resistance species that have blocked "killing" mechanisms, but little is known about herbistatics as there are so few, and whether they have select advantages over herbicides [*i.e.* as do some bacteriostatics (*e.g.*, clindamycin[20]) over bactericides]. To that end, the herbicide metsulfuron methyl (MM) (**8**) was chosen as a model template to explore herbistasis. MM is a highly potent broad-spectrum herbicide (Fig. 2), and a member of the sulfonylurea herbicide class.[21] This herbicide is a powerful inhibitor of acetolactate synthase (ALS) [also known as acetohydroxyacid synthase (AHAS)], which is the first enzyme in the branched-chain amino acid biosynthesis pathway and critical to plant growth.[22–25] Furthermore, anecdotal reports claim that MM limits plant growth at sub-lethal dosages without affecting the biomass through its ability to limit cell division.[26] Consequently, it may already have structural features conducive to herbistatic influences.

Reported herein is the utilisation of cyclooctatetraene (COT, **9**),[27,28] as a more dynamic biological probe to pursue any underlying herbistatic properties of MM through the synthesis of COT-MM (**10**). The COT ring system has previously been deployed as a phenyl ring (**11**) bioisostere/biomotif.[27,28] However, unlike other phenyl ring bioisosteres, such as bicyclo[1.1.1]pentane, bicyclo[2.2.2]octane, and cubane,[29] the COT ring contains both steric and π character components. Furthermore, the COT ring system has shape shifting properties arising from the dynamic equilibrium that exists between ring inversion (*e.g.*, **12**), π-bond shifts, and to a much lesser extent valence tautomerization (*i.e.*, bicyclo[4.2.0]octatriene **13**, and corresponding **14**) (Fig. 2).

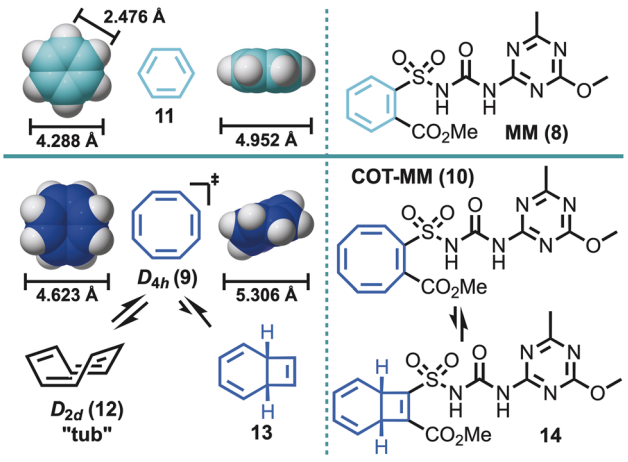

Fig. 2 Left panel, a bioisostere comparison between a phenyl ring (**11**) and cyclooctatetraene (COT, **9**) demonstrating geometric differences using space filling models shown in two different orientations [M06-2X/6-311+G(d,p)], along with the valence tautomerization of COT to an alternative isomer (**13**). Right panel, the herbicide, metsulfuron methyl (MM, **8**) and COT derivative (COT-MM, **10**) and the corresponding selected valence isomer (**14**).

Results and discussion

Synthesis of COT-metsulfuron methyl

Given that 1,2-disubstituted cyclooctatetraenes are best obtained from the photochemical reaction of acetylenes in the presence of benzene,[30] this approach was actively pursued. However, a suitably substituted acetylene (*i.e.*, **15**) was necessary for the installation of the methyl ester functional group, and to provide a connection point to the eventual sulfonylurea moiety. To achieve this goal, vinyl trimethyl silane (**16**) was generated from vinyl magnesium bromide (**17**),[31] followed by phosphorus tribromide mediated hydrobromination, to give **18**.[32] Alternatively, **18** could be synthesised *via* Appel reaction from commercially available 2-(trimethylsilyl)ethan-1-ol. Bromide **18** was then reacted with the *in situ* generated thiolate **19**,[33] derived from trimethylsilyl acetylene (**20**), to give the disubstituted acetylene **21** in 52% yield. Lithium metal exchange using methyl lithium complex[34] followed by quenching with methyl chloroformate gave smooth conversion of **21** to the ester **22**. The last step in the sequence consisted of oxidising the disulfide to the sulfone **15** with dimethyldioxirane (Scheme 1). Photolysis (254 nm) of acetylene **15** in the presence of benzene afforded the desired 1,2-disubstituted cyclooctatetraene (**23**) in moderate yield (25%).

Silyl deprotection of the sulfone (**23**), followed by conversion of the intermediate sulfinic acid to the sulfonamide **24** was achieve in 60% yield.[35] To introduce the urea functionality and complete the synthesis, sulfonamide **24** was reacted with phenylcarbamate (**26**), derived from 1,3,5-triazin-2-amine (**25**), to provide COT-MM (**10**) in 37% yield (Scheme 1).

Synthesis of COT-benthiocarb

In the view that the COT ring system is known to react with singlet oxygen, *via* the COT valence tautomer **13** (Fig. 2), to give an endoperoxide **27** (Scheme 2a),[36] and that plants produce singlet oxygen,[37] an alternate COT-herbicide control was required. That is, a control was required to ensure that any

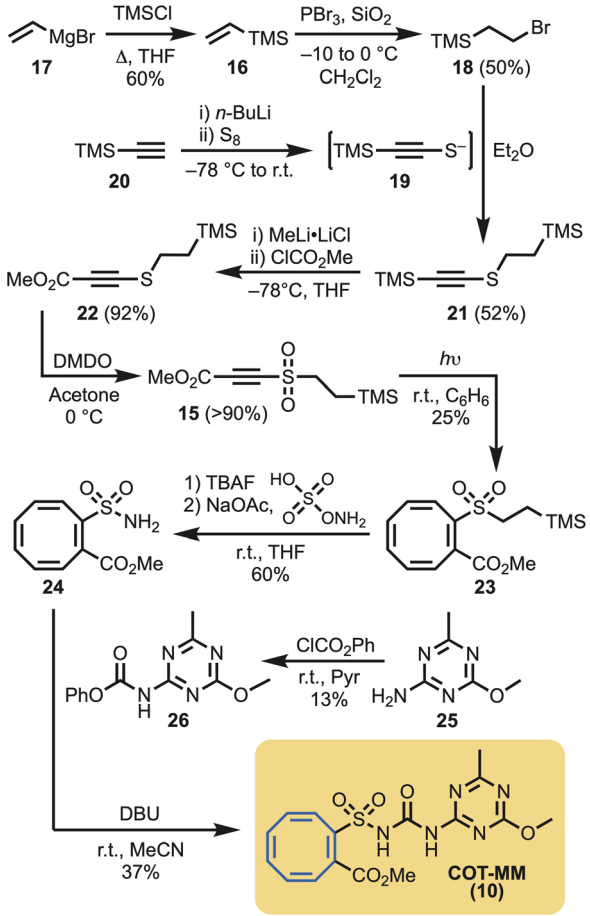

Scheme 1 Synthesis of COT-metsulfuron methyl (COT-MM, **10**).

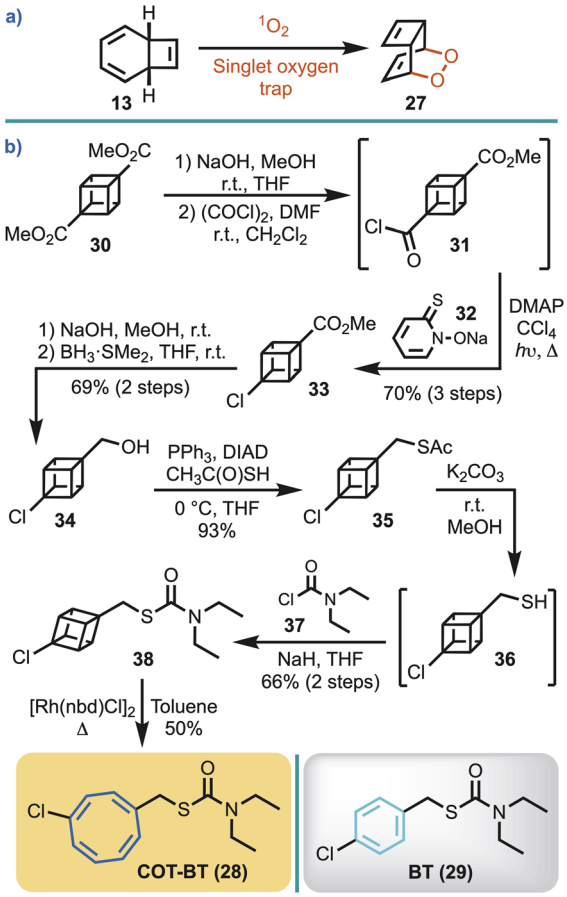

Scheme 2 (a) Reaction of singlet oxygen with COT *via* the valence tautomer. (b) Synthetic route employed to access COT-BT (**28**), with its parent herbicide BT (**29**) also shown.

observable herbistatic behaviour with COT-MM (**10**) was not caused by spurious plant singlet oxygen or plant P_{450} oxidation.[38] For this, the commercial herbicide benthiocarb [BT, (**29**)][39] was selected for phenyl ring replacement by COT to make COT-BT (**28**) (Scheme 2b). Importantly, the MOA for BT is through inhibition of long-chain fatty acid biosynthesis,[39–41] which should minimise potential enzyme cross-reactivity to ensure any observable effects are from its structural COT components, and not the direct inhibition of ALS.

In the view that 1,4-disubstituted COT ring systems are most efficiently obtained by rhodium catalysed valence isomerisation of 1,4-disubstituted cubanes,[42] this strategy was adopted for the synthesis of COT-BT. Half hydrolysis of cubane diester **30** was performed with sodium hydroxide, and the resulting acid converted to the corresponding acid chloride (**31**).[43] Barton chlorination, using **32**, gave **33** on irradiation in carbon tetrachloride. Subsequent hydrolysis, followed by borane reduction, gave the cubane alcohol **34**.[42] Conversion to the thioacetate **35** proceeded smoothly using a Mitsunobu reaction.[44] The thioacetate was then hydrolysed to thiol **36**, and subsequent exposure to sodium hydride followed by treatment with *N*,*N*-dimethylcarbamoyl chloride (**37**) afforded **38** in 66% yield. COT-BT (**28**) was then simply obtained through gentle heating of **38** in toluene at 60 °C using the commercially available rhodium(I) catalyst $[Rh(nbd)Cl]_2$ (Scheme 2b).

Plant biology

COT-MM and COT-BT were evaluated alongside their commercial relatives MM and BT against the Australian Weed of National Significance, *Cryptostegia grandiflora* (rubber vine). Rubber vine is regarded as one of Australia's worst weeds. It smothers native vegetation, forms dense thickets, and its invasiveness means it has the potential for further spread. This species is described as a climbing woody dicot, is native to Madagascar, and is now distributed widely throughout subtropical and tropical regions of the world.[45]

Initially, an *in vitro* study was performed over an 18 day post treatment period to assess the plant growth inhibition of COT-MM and COT-BT in relation to their corresponding commercial herbicides MM and BT (*i.e.* phenyl ring containing). Compared to the vehicle control, the application of MM and COT-MM reduced plant vertical growth by 100% and 96%, respectively (Fig. 3a). By comparison, treatment using COT-BT resulted in no reduction in growth, and BT by only 21% compared to the negative vehicle control (Fig. 3a).

Application of both MM and COT-MM led to a statistically significant decrease of 15% in shoot dry biomass (SDB), while root dry biomass (RDB) remained unaffected by these treatments. COT-BT showed no significant effect on any plant

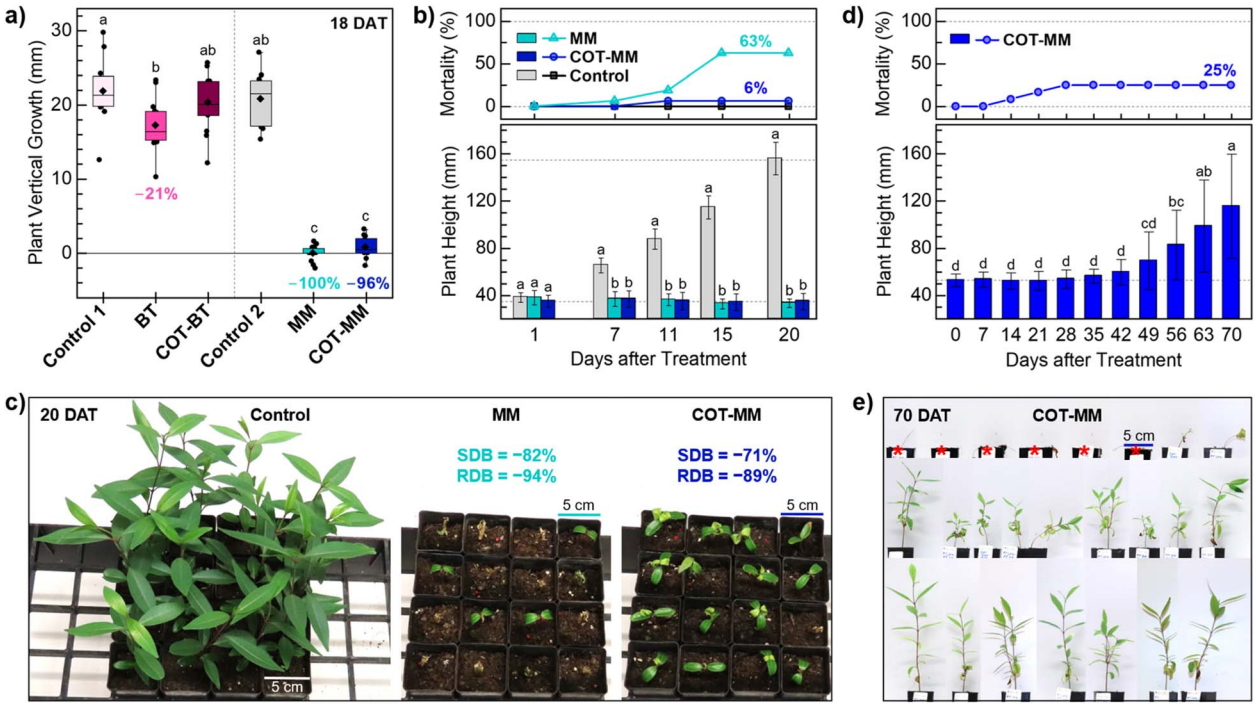

Fig. 3 The effect of COT-MM and COT-BT on vertical growth of rubber vine *in vitro* (a) and grown under glasshouse conditions (b–e). (a) The experiment was conducted over 18 days and the results (plant height 18 DAT–1 DAT) are compared to the commercial herbicides MM and BT and two vehicle only controls. Control 1 (1% DMSO, 1% Tween 80), BT (0.1 mM BT, in 1% DMSO, 1% Tween 80), COT-BT (0.1 mM COT-BT, in 1% DMSO, 1% Tween80), Control 2 (1% Tween 80), MM (0.1 mM MM K^+ in 1% Tween 80), and COT-MM (0.1 mM COT-MM K^+ in 1% Tween 80). $n = 13$ independent replicates. The diamond symbol represents the mean, the horizontal line represents the median, the box represents interquartile range (IQR), and the whiskers represent 1.5 × IQR. (b) Plant mortality over time (top) and the impact on rubber vine height (bottom), with reference lines at 35 mm and 155 mm, $n = 16$ independent replicates. Control (0.10 mM K_2CO_3 in 1% Tween 80), MM (0.10 mM MM K^+ in 1% Tween 80), and COT-MM (0.10 mM COT-MM K^+ in 1% Tween 80) measured periodically over 20 DAT. (c) The visual effects of treatments on rubber vine plants 20 DAT, and the relative impact on shoot dry biomass (SDB) and root dry biomass (RDB) for MM and COT-MM compared to the control. (d) Long-term impact of chemical treatment of COT-MM on rubber vine grown under glasshouse conditions. Rubber vine plants ($n = 24$) were treated with COT-MM (0.1 mM COT-MM K^+ in 1% Tween 80) and the plant height and plant mortality were recorded weekly from 0 to 70 DAT. (e) The visual effects of the treatment on the rubber vine plants at 70 DAT grown in 5 cm square pots. Dead plants ($n = 6$) marked with red asterisk. For (a), (b), and (d) the different letters above columns indicate significant differences in average plant height over time ($p < 0.05$, Tukey's HSD test), error bars represent the standard deviation, and data points outside the whiskers represent outliers. [Note: due to the instability of sulfonylurea functional groups in dimethylsufoxide (DMSO), conversion of COT-MM (and MM) to its potassium salt was necessary to improve aqueous solubility for plant experiments and enzymatic assays (see ESI†)].

growth parameter assessed, and BT did not significantly impact SDB or RDB (Fig. S1 and Table S1, ESI†). Both negative control treatments (1% DMSO with 1% Tween 80, and 1% Tween 80) also demonstrated indistinguishable effects on plant vertical growth, as well as on SDB and RDB (Table S1, ESI†).

In a subsequent glasshouse study, the effect of COT-MM was compared with that of MM over a 20 day post-treatment period, with both demonstrating a statistically significant negative impact on rubber vine growth (Fig. 3b) (Table S2 and Fig. S2, ESI†). Control-treated (*i.e.*, K_2CO_3 added) plants exhibited a 4-fold increase in vertical growth from 0 to 20 days after treatment (DAT) (from roughly 35 mm to 150 mm), whereas plants treated with MM and COT-MM remained the same height as when first treated (Fig. 3b). A mortality rate of 6% for plants treated with MM was observed at 7 DAT, which increased to 19% at 11 DAT, and peaked at 63% by 15 DAT.

Comparably, treatment with COT-MM induced a 6% mortality rate from 11 DAT, but this remained constant until the end of the experiment at 20 DAT. Control-treated plants displayed no mortality through the duration of the experiment (Fig. 3b).

Shoot and root dry biomass (SDB, RDB) were equally and significantly affected by MM and COT-MM at 20 DAT compared to the control. MM and COT-MM reduced SDB by 82% and 71%, respectively, and RDB was decreased by 94% and 89%, respectively (Fig. 3c, Table S2 and Fig. S2, ESI†).

The experimental outcomes reported above support the view that COT-MM is a herbistatic agent, as the inhibition to plant growth was no longer observed to be comorbid with plant death, as is typical of most commercial herbicides. Applying MM and COT-MM at concentrations ranging from 0.01 mM to 0.40 mM showed comparable behaviour in respect to both plant vertical growth and RDB, with minor variation to SDB as a function of concentration (Table S3 and Fig. S3, ESI†). Minimal effects to rubber vine plants grown *in vitro* from BT and COT-BT indicates that the inclusion of the COT functional group did not have an

influence on plant singlet oxygen or plant P_{450} oxidation pathways.

A longer-term glasshouse study was performed with COT-MM to determine the extent of herbistasis, and whether it was reversible. Rubber vine mortality was observed to peak at 25% at 28 DAT and remained constant until the end of the experiment at 70 DAT (Fig. 3d and e). Similarly to the 20 day glasshouse study, no plant death was observed within the first 7 DAT, and a comparable 8% mortality rate was observed at 14 DAT. While no plant death was observed after 28 DAT, the 18 surviving plants exhibited stunted vertical growth up to 42 DAT, with the first noticeable increase in height measured at 49 DAT. By 56 DAT plant height had increased by 57% compared to the height at the time of treatment (0 DAT), rising to 87% at 63 DAT, and reaching 119% at the end of the experiment at 70 DAT (Fig. 3d). These results provide additional support that COT-MM is a herbistatic agent, as rubber vine plants appear to recover after sustaining more than six weeks of inhibited growth (Fig. S4, ESI†).

Enzymology

ALS catalyses the conversion of two molecules of pyruvate into 2-acetolactate, or one molecule of pyruvate and one molecule of 2-ketobutyrate into 2-aceto-2-hydroxybutyrate: essential precursors for the biosynthesis of branched chain amino acids (BCAA). Magnesium coordinated thiamine diphosphate ($ThDP{\cdot}Mg^{2+}$) and flavin adenine dinucleotide (FAD) are cofactors required for this process. However, excess molecular oxygen can cause enzyme dysregulation and the production of peracetate through a side-reaction involving the ThDP-hydroxyethyl intermediate.[22–25]

To test whether COT-MM has the same MOA as its parent template MM, a detailed kinetic study was performed (Fig. 4). The ALS from *Arabidopsis thaliana* (*At*ALS) was chosen as a model enzyme on which to perform inhibition studies. Its sequence identity and sequence homology with rubber vine ALS are 82.1% and 96.4%, respectively. The amino acids in the herbicide binding site are also completely conserved (Fig. S5, ESI†). This therefore represents an excellent interpretative model for analysis.

The inhibition assay was performed after nitrogen purging of the master solution to minimize any effects of the side-reaction involving molecular oxygen. The continuous assay method was applied to monitor the disappearance of pyruvate directly and to determine when the lag phase of the reaction had been completed. Initial testing showed that MM was an extremely tight binding inhibitor while COT-MM was a weak binding inhibitor, and therefore required a different range of inhibitor concentrations between the two experiments (Fig. 4). Applying the tight binding equation (eqn (S2), ESI†) a K_i value of 47 nM was obtained for MM (Fig. 4a), which is a similar value to that previously published (80 nM)[46] taking into account a discontinuous assay was used for the latter value. A K_i value of 19 mM was obtained for COT-MM (Fig. 4b), but since tight binding was not observed, the equation for non-competitive inhibition was used (eqn (S1), ESI†).[25] No inhibition of *At*ALS was observed for BT or COT-BT, as was expected since the target of BT is reported to be long-chain fatty acid biosynthesis.[39–41]

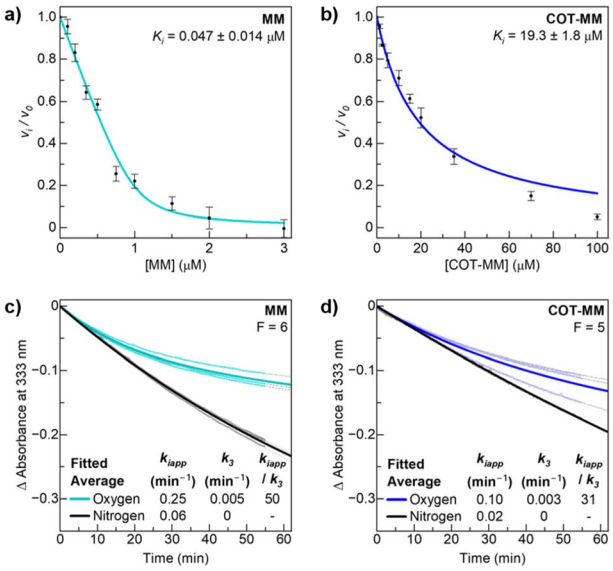

Fig. 4 Inhibition plots of MM and COT-MM for *At*ALS. K_i measurement of (a) MM fitted with the tight binding equation, and (b) COT-MM fitted with the simple inhibition equation. The time-dependent accumulative inhibition curves at 25 °C for (c) MM and (d) COT-MM, under normal oxygen aerobic conditions (teal and blue respectively), and nitrogen anaerobic conditions (black). The individual replicates are fitted with grey dotted lines, and the averaged fitted curves (bolded lines) use the respective F values ($[E]_F/[EI]$) and eqn (S3) (ESI†) to determine the average values of k_{iapp} and k_3. All measurements were performed in triplicate with error bars representing the standard deviations (SD) of the data.

Next, the accumulative inhibition of *At*ALS by MM and COT-MM was measured under standard aerobic conditions as well as after nitrogen purging to investigate the influence of dissolved oxygen on the inhibition kinetics. The key values for the assessment of accumulative inhibition are the apparent rate of inactivation in the presence of the inhibitor (k_{iapp}), and the enzyme recovery rate that occurs in the absence of inhibitor (k_3) ((eqn (S3) and Fig. S6, ESI†).[25] These values are dependent on the ratio of free enzyme to inhibitor–enzyme complex, so were kept similar in all experiments by determining the F value from the K_i values and eqn (S4) (see ESI† for details).

Under aerobic assay conditions, the k_{iapp}, k_3, and k_{iapp}/k_3 values for MM were 0.25 min^{-1}, 0.005 min^{-1}, and 50 respectively, and for COT-MM they were 0.10 min^{-1}, 0.003 min^{-1}, and 31, respectively (Fig. 4c, d and Table S4, ESI†). The higher k_{iapp}/k_3 for MM suggests a slower recovery rate, and therefore an increase in accumulative inhibition. The decreased k_{iapp} value for COT-MM compared to MM was initially suspected to arise from the reactive oxygen quenching abilities of COT (Scheme 2a) protecting ThDP and $FADH_2$ from oxidative inactivation. However, no oxygenated COT-MM by-products were detected by mass spectrometry (see below), hence it is likely that this may result from a modified inhibitor orientation within the active site (see below).

To further explore the importance of oxygen towards ALS enzyme inhibition, the master solution was purged with

nitrogen and supplemented with the known oxygen quenching reagent, 2-mercaptoethanol, to simulate anaerobic conditions. No time-dependent inhibition could be measured for COT-MM or MM under deoxygenated conditions ($k_3 = 0$), and both displayed a 5-fold decrease of k_{iapp} to 0.06 min^{-1} and 0.02 min^{-1}, respectively (Fig. 4c and d). The maximum enzyme velocity (V_{max}) was constant across all samples (Table S4, ESI†). The apparent non-reversible inhibition under deoxygenated conditions is tentatively suggested to result from degradation of ThDP through the physical aspects of competitive/non-competitive inhibition when MM and COT-MM occupy the enzyme active site. This contribution to ALS inhibition is likely still present under oxygenated conditions, although only a minor component compared to the dominating accumulative pathway.

In a subsequent experiment the reaction temperature was increased from 25 °C to 30 °C to investigate the relative inhibition rates with elevated V_{max} at temperatures closer to those of glasshouse plant experiments (Table S4 and Fig S7, ESI†). The five degree increase in temperature approximately doubled the V_{max}, and the k_{iapp} under aerobic conditions was also doubled to 0.57 min^{-1} for MM, and to 0.23 min^{-1} for COT-MM. The enzyme recovery rate in the absence of inhibitor again appeared equivalent under oxygenated conditions between COT-MM and MM ($k_3 = 0.02$ min^{-1}), and an order of magnitude higher than that at 25 °C. It is important to note that this recovery rate represents holoenzyme and [ES*] → [ES$^{\#}$] (after [ES*I] → [ES*]), and not the original enzyme without cofactors (Fig. S6, ESI†). As the experimental methods and consistent F values ensure that the observed rate constants were derived at equivalent [ESI] concentrations, inhibitors with the same binding inhibition mechanism should also demonstrate comparable k_3 values. Therefore, COT-MM and MM are expected to act *via* the same mechanism, as would be expected due to their similar chemical composition and that ALS herbicides do not typically induce structural changes to the enzyme active site as a consequence of herbicide inhibition.

While the addition of 2-mercaptoethanol was not found to influence the binding affinity or K_i values of MM or COT-MM (data not shown), it was omitted under nitrogen sparged conditions at 30 °C. As was expected, COT-MM again did not display any accumulative inhibition ($k_3 = 0$), with a k_{iapp} of 0.02 min^{-1}. Notably, this k_{iapp} value is the same as the 25 °C-condition using 2-mercaptoethanol, supporting the theory that ThDP degradation *via* physical inhibition is dominating under anaerobic conditions, with minimal contribution from reactive oxygen pathways (Table S4 and Fig S7, ESI†). Any oxygen quenching from the COT ring in the absence of 2-mercaptoethanol is assumed to be minimal. A small amount of accumulative inhibition was observed for MM in the nitrogen sparged condition ($k_{iapp}/k_3 = 5$), which may be due to the fact that MM is an extremely tight binder, and that residual oxygen is likely remaining in the system. The *At*ALS binding affinity of MM (47 nM) is almost 500 times stronger than COT-MM (19 mM), so it is anticipated that this variation to binding affinity would also modify the ability to trap reactive oxygen species.

The lower K_i and lower k_{iapp} values of COT-MM across the kinetic experiments indicates a decreased active site presence in *At*ALS compared to MM. Nevertheless, plant experiments using equal concentrations of COT-MM and MM (*i.e.* 0.05, 0.20 and 0.40 mM) showed comparable inhibition to plant growth (Fig. S3, ESI†). This highlights that oxidative inactivation of this enzyme is a potent mode of action, which could dominate over the herbicide binding affinity and the apparent rate of enzyme inactivation as the leading predictor of herbicide activity. Coincidentally, the reported rate of enzyme activation ($k_{obs(act)}$)[47] for WT *At*ALS is comparable to the k_{iapp} observed for COT-MM under 30 °C aerobic conditions. This serendipitous result corroborates the observed herbistatic behaviour under glasshouse conditions, with BCAA production at steady state due to the ALS inactivation rate from COT-MM being equal to its intrinsic reactivation rate. In plants, this could sustain the essential biological functions by constant BCAA production, but prevent further plant growth due to restricted output. It is assumed that this inhibition mechanism would persist until the inhibitor is metabolised or degraded, or until secondary processes result in plant death. The k_{iapp} for MM at both 25 °C and 30 °C is higher than the enzyme reactivation rate (*i.e.*, $k_{iapp} > k_{obs(act)}$), so the enzyme equilibrium moves towards the inactivated "off" state, yielding accumulative inhibition and increased plant death.

Mass spectrometry

A mass spectroscopic study was performed to discover if the herbistatic effect from COT-MM originates from oxidative side reactions within the enzyme active site. For example, representative oxidised products such as **39** and **40** (Fig. 5) could be produced if the COT moiety reacted with peracetate or singlet oxygen, as previously observed for ALS.[22–24] Samples for mass spectroscopic analysis were prepared similarly to those for the

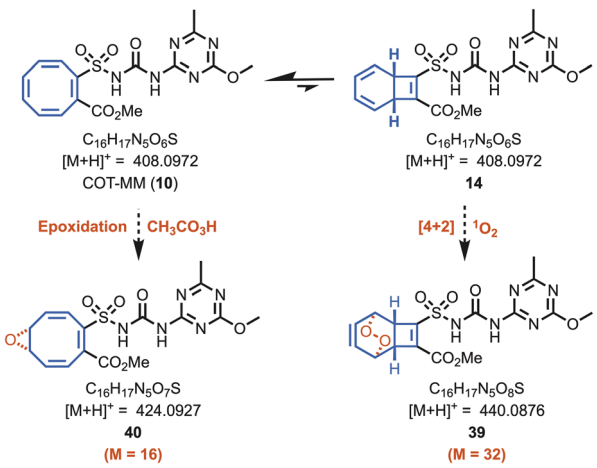

Fig. 5 Molecular masses of potential oxidation products of COT-MM. Potential products **40** and **39** arising from oxidation of COT-MM by either peracetic acid, or singlet oxygen, respectively. No peaks corresponding to the expected molecular masses of **39** and **40** were observed by mass spectrometry when searching the extracted-ion chromatogram (XIC) by their respective chemical formulas.

kinetic assays containing COT-MM and MM at 30 °C. Experimental controls involved performing the *At*ALS reaction with and without inhibitor, as well as comparison to inhibitor only samples. The *At*ALS reactions were sampled at 1 and 12 hours to provide sufficient time for enzyme inhibition and potential side reactions to occur. Compared to the plain enzyme control, no new products were detected for COT-MM or MM. The peak retention time for the extracted-ion chromatogram (XIC) of COT-MM (*m*/*z* 408.0972) remained identical across the different time points, indicating no detectable oxidation of the COT ring system (Fig. S8, ESI†). That is, no mono- or di-oxygen atom additions to COT-MM were observed, as would be expected for their corresponding molecular ions associated with the molecular masses of **39** and **40**. Similarly, no new peaks were observed for MM (Fig. S9, ESI†). Under all sampled conditions, a predominating peak for the inhibitors was observed, which had comparable intensity and retention time to the inhibitor-only conditions. COT-MM and MM are therefore chemically stable and are not significantly metabolised or modified under the *in vitro* enzyme inhibition experimental conditions.

Molecular docking

A crystal structure of the complex between *At*ALS and COT-MM could not be obtained, despite extensive efforts. Nevertheless, molecular docking using *At*ALS was performed and showed that COT-MM likely occupies a position similar to that of MM and other commercial ALS-inhibiting herbicides, especially regarding the heterocyclic ring and the sulfonylurea bridge (Fig. 6, S10 and S11, ESI†). Another feature common to the sulfonylureas when binding to ALS is that they adopt a bent "U" or "L" shape with respect to the location of the heterocyclic ring and the aromatic ring. This is indeed the case for MM (Fig. 6a). However, the docking of COT-MM suggests that it may favour a fully extended structure, likely due to the increased size of the COT ring (**12**, Fig. 2) preventing it from slotting into the location where the aromatic ring of MM binds. The loss of aromaticity due to the replacement of the phenyl ring with the COT ring also takes away the opportunity for stabilising π–cation interactions, instead having possible interactions to residues at the entrance to the active site such as a salt bridge with R199 or hydrophobic interactions with P197 and K256 (Fig. S12, ESI†). In the docked structure, the heterocycle of COT-MM forms a π–π stacking arrangement with W574, and the sulfonylurea linker forms hydrogen bonds with the backbone carbonyl of G121 and with the sidechains of R377, S653, and K256 (Fig. 6b). These interactions are consistent with the binding mode of MM and other sulfonylurea herbicides whose structures have been determined in complex with *At*ALS.[48–50] Furthermore, the docked binding orientation of COT-MM relative to FAD and ThDP-peracetate side-product is comparable to that of MM, indicating sufficient space is available for the oxygenase side-reaction and therefore time dependent accumulative inhibition to occur.

However, the higher k_{iapp}/k_3 ratio for MM suggests increased accumulative inhibition, likely due to its decreased size and compact bent configuration (Fig. 6a). Therefore, it was considered that the enzyme—MM complex can more readily trap the reactive ThDP-carbanion intermediate without access to a second acceptor keto-acid that is required for product formation. Analogous to the previously proposed "waiting room" theory,[51] where both donor and acceptor keto-acids are bound simultaneously in the initial stages of the reaction. Closure of the active site after MM binds prevents further exchange with solvent or substrate, leaving the ThDP-carbanion exposed and susceptible to degradation or side-reactions.[22] Consequently, oxygenation within the enzyme—MM complex can cause the formation of ThDP-peracetate, which then oxidises $FADH_2$ to the inactive FAD form, with re-reduction by pyruvate oxidase for enzyme activation being the rate limiting step ($k_{obs(act)} = 0.2\ min^{-1}$ for *At*ALS).[47] A comparable process is postulated to occur for the enzyme–COT-MM complex, however its extended structure may allow the active site to stay open, enabling the migration of oxygen or keto-acids and decreasing the possibility of ThDP-peracetate formation. As reflected by the increased K_i, the loss of stabilizing phenyl ring interactions may also prevent the ThDP-peracetate side-product from being constrained in the correct orientation for reaction with $FADH_2$. While the lower k_{iapp} values of COT-MM compared to MM demonstrates less efficient enzyme inactivation, the exact mechanism behind accumulative inhibition is yet to be confirmed. However, both the molecular docking and the time-dependent enzyme kinetic studies strongly suggest the target for the herbistasis activity of COT-MM is through the inhibition of ALS.

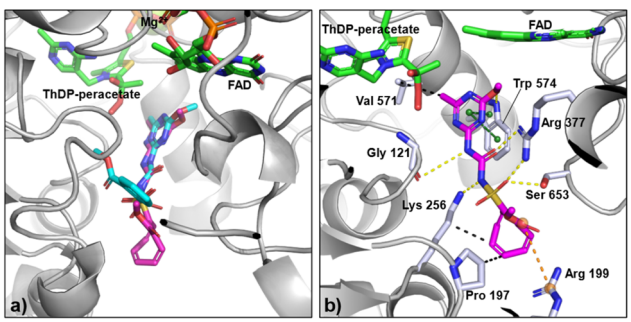

Fig. 6 Binding mode of MM and COT-MM to *At*ALS. (a) Crystal structure of MM (cyan, PDB:1YHY) in complex with *At*ALS (grey) and cofactors (green), overlayed with the docking pose of COT-MM (magenta). (b) Docking pose of COT-MM with ligand interactions to residues (pale blue), by hydrogen bonds (yellow dashes), π–π stacking (green dashes), salt bridge (orange dashes), and hydrophobic interactions (black dashes). Nitrogen atoms in dark blue, sulfur in yellow, and oxygen in red.

Conclusions

In summary, plant cell division reportedly ceases shortly after application of MM, and plant death occurs one to three weeks after application depending on the dosage, weed species, and environmental conditions.[52] In this study, under both *in vitro* and glasshouse conditions, the vertical growth of rubber vine was observed to be halted almost immediately after the application of both COT-MM and MM. Unlike MM however, the mortality rate (6%) stayed constant for those plants treated with

COT-MM over a 20 day post treatment period. When a longer-term study was undertaken and COT-MM treated plants were monitored for 70 days, the mortality increased until day 28, plateauing at 25%. The plants were then observed to remain in a state of herbistasis for an additional three weeks, with a statistically significant increase to plant height first detected at day 56 (*i.e.*, eight weeks after treatment). The plants continued to increase in height for the remainder of the experiment, with a 119% increase to plant height on day 70 compared to when first treated (Fig. 3).

This observation is remarkable in that the ALS inhibition MOA is the same as MM as confirmed by *At*ALS kinetics, and supported by molecular docking, but the mechanism of action has switched from herbicidal to herbistatic for COT-MM. Mass spectroscopy, and the COT moiety control agent, COT-BT, suggests the herbistasis effect is not the result of oxidative modification of COT-MM due to plant or ALS reactive oxygen species. Molecular docking reveals that the COT-MM adopts a fully extended structure compared to that for the other sulfonylureas and MM, with the COT moiety in the "tub-shaped" conformation (D_{2d}) (Fig. 2) expanding beyond the binding access channel. This supports why COT-MM does not bind as tightly to *At*ALS as MM, enabling it to move in and out of the binding channel more freely. This would result in a decrease in BCAA synthesis, rather than the potent decrease which occurs for tight binding inhibitors such as MM.

Inducing plant herbistasis is rare, and even more so for synthetic chemicals. As explored herein, the herbistatic features displayed by COT-MM were realised by targeting the well-established ALS MOA and applying a bioisostere/biomotif chemical modification protocol using a pre-existing commercial herbicide template. Deploying these methods to reinvigorate the concept of herbistasis could provide additional tools for tackling the weed crisis. For example, (1) weeds may need to evolve alternate mechanisms of resistance, which would potentially prolong resistance development; or (2) the low-mortality and herbistasis induced by COT-MM could be employed in combination with weed biocontrol agents at crucial times of the weed lifecycle to suppress plant growth and seed set while enabling the agent population to persist on the weed in the environment. Lastly, potential applications outside of weed control can also be envisaged, such as placing crop seedlings into stasis to avoid the impact of impending deleterious weather like drought.

Data availability

All experimental data are provided in the ESI.†

Author contributions

G. P. S., G. H. W., M. A. R., L. W. G., and C. M. W. designed and coordinated the research. H. X., S. K. M. M., I. S. J. S., Y. L., S. C., T. F.-J., and S. D. H. performed chemical synthesis, characterisation, and solubility studies. B. D. B., C.-E. M., and R. M. H. performed plant assays. C. W., S.-H. H., T. L., A. N., Q. Z., J. M. B. performed enzyme kinetics, docking and mass spectrometry. C. M. W. wrote the manuscript with input from all authors.

Conflicts of interest

There are no conflicts to declare.

Acknowledgements

The Australian Government, through the Department of Agriculture and Water Resources (CT-06) and the Department of Agriculture, Fisheries and Forestry, is gratefully acknowledged for funding to C. M. W., G. H. W., M. A. R. and L. W. G. We also thank the University of Queensland (UQ) and the Commonwealth Scientific and Industrial Research Organisation (CSIRO, Melbourne and Brisbane) for institutional support, and Boron Molecular Pty Ltd for dimethyl cubane-1,4-dicarboxylate. Ms Kelli Murree from the Queensland Government, Department of Agriculture and Fisheries, Tropical Weeds Research Centre, is gratefully acknowledged for collection of rubber vine seeds. Mr Tim J. Vance is gratefully acknowledged for assistance with the long term rubber vine plant experiment.

Notes and references

1 C. Herbicides, *Efficacy, Toxicology, and Environmental Impacts*, ed. R. Mesnage and J. G. Zaller, Elsevier, 2021.
2 S. O. Duke and F. E. Dayan, Herbicides, *eLS*, 2018, 1–9.
3 J. Clapp, Explaining Growing Glyphosate Use: The Political Economy of Herbicide-Dependent Agriculture, *Glob. Environ. Change*, 2021, **67**, 102239.
4 C. J. Hall, E. R. R. Mackie, A. R. Gendall, M. A. Peruginia and T. P. Soares da Costa, Review: amino acid biosynthesis as a target for herbicide development, *Pest Manag. Sci.*, 2020, **76**, 3896–3904.
5 R. Ofosu, E. D. Agyemang, A. Márton, G. Pásztor, J. Taller and G. Kazinczi, Herbicide Resistance: Managing Weeds in a Changing World, *Agronomy*, 2023, **13**, 1595.
6 H. J. Beckie, Herbicide Resistance in Plants, *Plants*, 2020, **9**, 435.
7 T. A. Gaines, R. Busi and A. Küpper, Can new herbicide discovery allow weed management to outpace resistance evolution?, *Pest Manag. Sci.*, 2021, **77**, 3036–3041.
8 S. Hachisu, Strategies for discovering resistance breaking, safe and sustainable commercial herbicides with novel modes of action and chemotypes, *Pest Manag. Sci.*, 2021, **77**, 3042–3048.
9 S. O. Duke and F. E. Dayan, The search for new herbicide mechanisms of action: Is there a 'holy grail'?, *Pest Manag. Sci.*, 2022, **78**, 1303–1313.
10 B. He, Y. Hu, W. Wang, W. Yan and Y. Ye, The Progress towards Novel Herbicide Modes of Action and Targeted Herbicide Development, *Agronomy*, 2022, **12**, 2792.
11 T. P. Selby, A. D. Satterfield, A. Puri, T. M. Stevenson, D. A. Travis, M. J. Campbell, A. E. Taggi, K. A. Hughes and J. Bereznak, Bioisosteric Tactics in the Discovery of

Tetflupyrolimet: A New Mode-of-Action Herbicide, *J. Agric. Food Chem.*, 2023, **71**, 18197–18204.
12 F. R. West Jr and J. H. M. Henderson, A Turbidimetric Method for Determining the Effect of 2,4-D Upon the Growth of Yeast, *Science*, 1948, **107**, 604.
13 P. A. Grieco, D. J. Morre, T. H. Corbett and F. A. Valeriote, Therapeutic quassinoid preparations with antineoplastic, antiviral, and herbistatic activity, *US Pat.*5965493(PCT/US95/14321), 1999.
14 S. Bowe, M. Landes, J. Best, G. Schmitz and M. Graben, BAS 662 H: an innovative herbicide for weed control in corn, *1999 Brighton crop protection conference weeds proceedings of an international conference*, Brighton, UK, 15–18 November 1999, vol. 1, pp. 35–40.
15 S. Inman and S. Semones, Methods of controlling weeds with thaxtomin and thaxtomin compositions in combination with a beneficial herbicide, WO2013/066894A3(PCT/0S2012/062615), 2013.
16 T. Asami, Y. K. Min, N. Nagata, K. Yamagishi, S. Takatsuto, S. Fujioka, N. Murofushi, I. Yamaguchi and S. Yoshida, Characterization of Brassinazole, a Triazole-Type Brassinosteroid Biosynthesis Inhibitor, *Plant Physiol.*, 2000, **123**, 93–99.
17 K. Oh, T. Matsumoto, A. Yamagami, T. Hoshi, T. Nakano and Y. Yoshizawa, Fenarimol, a pyrimidine-type fungicide, inhibits brassinosteroid biosynthesis, *Int. J. Mol. Sci.*, 2015, **16**, 17273–17288.
18 M. C. Fisher, A. Alastruey-Izquierdo, J. Berman, T. Bicanic, E. M. Bignell, P. Bowyer, M. Bromley, R. Brüggemann, G. Garber, O. A. Cornely, S. J. Gurr, T. S. Harrison, E. Kuijper, J. Rhodes, D. C. Sheppard, A. Warris, P. L. White, J. Xu, B. Zwaan and P. E. Verweij, Tackling the emerging threat of antifungal resistance to human health, *Nat. Rev. Microbiol.*, 2022, **20**, 557–571.
19 N. Shetty, E. Aarons and J. Andrews, Chapter 5: General principles of antimicrobial therapy, in *Infectious Disease: Pathogenesis, Prevention and Case Studies*, ed. J. Andrews, N. Shetty and J. W. Tang, Wiley-Blackwell, 2009.
20 G. A. Pankey and L. D. Sabath, Clinical Relevance of Bacteriostatic versus Bactericidal Mechanisms of Action in the Treatment of GramPositive Bacterial Infections, *Clin. Infect. Dis.*, 2004, **38**, 864–870.
21 M. H. Russell, J. L. Saladini and F. Lichtner, Sulfonylurea herbicides, *Pestic. Outlook*, 2002, **13**, 166–173.
22 T. Lonhienne, A. Nouwens, C. M. Williams, J. A. Fraser, Y.-T. Lee, N. P. West and L. W. Guddat, Commercial Herbicides Can Trigger the Oxidative Inactivation of Acetohydroxyacid Synthase, *Angew. Chem., Int. Ed.*, 2016, **55**, 4247–4251.
23 T. Lonhienne, M. D. Garcia, C. Noble, J. Harmer, J. A. Fraser, C. M. Williams and L. W. Guddat, High Resolution Crystal Structures of the Acetohydroxyacid Synthase-Pyruvate Complex Provide New Insights into Its Catalytic Mechanism, *ChemistrySelect*, 2017, **2**, 11981–11988.
24 T. Lonhienne, Y. S. Low, M. D. Garcia, T. Croll, Y. Gao, Q. Wang, L. Brillault, C. M. Williams, J. A. Fraser, R. P. McGeary, N. P. West, M. J. Landsberg, Z. Rao, G. Schenk and L. W. Guddat, Structures of fungal and plant acetohydroxyacid synthases, *Nature*, 2020, **586**, 317–321.
25 M. D. Garcia, A. Nouwens, T. Lonhienne and L. W. Guddat, Comprehensive understanding of acetohydroxyacid synthase inhibition by different herbicide families, *Proc. Natl. Acad. Sci. U.S.A.*, 2017, **114**, E1091–E1100.
26 J. Bas Nelemans, R. P. A. van Wijingaarden, I. Roessink and G. H. P. Arts, Effects of the Herbicide Metsulfuron-Methyl on a Plant Community, Including Seed Germination Success in the F1 Generation, *Front. Environ. Sci.*, 2017, **5**, 10.
27 H. Xing, S. D. Houston, X. Chen, S. Ghassabian, T. Fahrenhorst-Jones, A. Kuo, C.-E. P. Murray, K.-A. Conn, K. N. Jaeschke, D.-Y. Jin, C. Pasay, P. V. Bernhardt, J. M. Burns, J. Tsanaktsidis, G. P. Savage, G. M. Boyle, J. J. De Voss, J. McCarthy, G. H. Walter, T. H. J. Burne, M. T. Smith, J.-K. Tie and C. M. Williams, Cyclooctatetraene: A Bioactive Cubane Paradigm Complement, *Chem.–Eur. J.*, 2019, **25**, 2729–2734.
28 S. D. Houston, T. Fahrenhorst-Jones, H. Xing, B. A. Chalmers, M. L. Sykes, J. E. Stok, C. F. Soto, J. M. Burns, P. V. Bernhardt, J. J. De Voss, G. M. Boyle, M. T. Smith, J. Tsanaktsidis, G. P. Savage, V. M. Avery and C. M. Williams, The Cubane Paradigm in Bioactive Molecule Discovery: Further Scope, Limitations and the Cyclooctatetraene Complement, *Org. Biomol. Chem.*, 2019, **17**, 6790–6798.
29 N. A. Meanwell, Applications of Bioisosteres in the Design of Biologically Active Compounds, *J. Agric. Food Chem.*, 2023, **71**, 18087–18122.
30 R. L. Grange, M. J. Gallen, H. Schill, J. P. Johns, L. Dong, P. G. Parsons, P. W. Reddell, V. A. Gordon, P. V. Bernhardt and C. M. Williams, [4+2] Cycloaddition Reactions Between 1,8-Disubstituted Cyclooctatetraenes and Diazo Dienophiles: Stereoelectronic Effects, Anticancer Properties and Application to the Synthesis of 7,8-Substituted Bicyclo [4.2.0]octa-2,4-dienes, *Chem.–Eur. J.*, 2010, **16**, 8894–8903.
31 A. Pollex and M. Hiersemann, Catalytic Asymmetric Claisen Rearrangement in Natural Product Synthesis: Synthetic Studies toward (−)-Xeniolide F, *Org. Lett.*, 2005, **25**, 5705–5708.
32 T. K. Tran, Q. Bricaud, M. Oçafrain, P. Blanchard, J. Roncali, S. Lenfant, S. Godey, D. Vuillaume and D. Rondeau, Thiolate Chemistry: A Powerful and Versatile Synthetic Tool for Immobilization/Functionalization of Oligothiophenes on a Gold Surface, *Chem.–Eur. J.*, 2011, **17**, 5628–5640.
33 W. W. Seidel, M. J. Meel, M. Schaffrath and T. Pape, Pursuit of an Acetylenedithiolate Synthesis, *Eur. J. Org Chem.*, 2007, 3526–3532.
34 L. Hoffmeister, T. Fukuda, G. Pototschnig and A. Fürstner, Total Synthesis of an Exceptional Brominated 4-Pyrone Derivative of Algal Origin: An Exercise in Gold Catalysis and Alkyne Metathesis, *Chem.–Eur. J.*, 2015, **21**, 4529–4533.
35 F. W. Monnard, E. S. Nogueira, T. Heinisch, T. Schirmer and T. R. Ward, Human carbonic anhydrase II as host protein for the creation of artificial metalloenzymes: the asymmetric

transfer hydrogenation of imines, *Chem. Sci.*, 2013, **4**, 3269–3274.

36 W. Adam, O. Cueto, O. De Lucchi, K. Peters, E.-M. Peters and H. G. Schnering, Synthesis of the endoperoxide anti-7,8-dioxatricyclo[4.2.2.$0^{2,5}$]deca-3,9-diene via singlet oxygenation of the bicyclic valence tautomer of cyclooctatetraene and its transformations, *J. Am. Chem. Soc.*, 1981, **103**, 5822–5828.

37 C. Triantaphylidés and M. Havaux, Singlet oxygen in plants: production, detoxification and signaling, *Trends Plant Sci.*, 2009, **14**, 219–228.

38 S.-M. C. Lau and D. P. O'Keefe, Analysis of herbicide metabolism by monocot microsomal cytochrome P450, *Method. Enzymol.*, 1996, **272**, 235–242.

39 Y. Tanetani, K. Kaku, M. Ikeda and T. Shimizu, Action mechanism of a herbicide, thiobencarb, *J. Pestic. Sci.*, 2013, **38**, 39–43.

40 C.-W. Chu, B. Liu, N. Li, S.-G. Yao, D. Cheng, J.-D. Zhao, J.-G. Qiu, X. Yan, Q. He and J. He, A Novel Aerobic Degradation Pathway for Thiobencarb Is Initiated by the TmoAB Two-Component Flavin Mononucleotide-Dependent Monooxygenase System in Acidovorax sp. Strain T1, *Appl. Environ. Microbiol.*, 2017, **83**, e01490.

41 N. G. Dimaano, T. Tominaga and S. Iwakami, Thiobencarb resistance mechanism is distinct from CYP81A-based cross-resistance in late watergrass (Echinochloa phyllopogon), *Weed Sci.*, 2022, **70**, 160–166.

42 S. D. Houston, H. Xing, P. V. Bernhardt, T. J. Vanden Berg, J. Tsanaktsidis, G. P. Savage and C. M. Williams, Cyclooctatetraenes through Valence Isomerization of Cubanes: Scope and Limitations, *Chem.–Eur. J.*, 2019, **25**, 2735–2739.

43 B. A. Chalmers, H. Xing, S. Houston, C. Clark, S. Ghassabian, A. Kuo, B. Cao, A. Reitsma, C.-E. P. Murray, J. E. Stok, G. M. Boyle, C. J. Pierce, S. W. Littler, D. A. Winkler, P. V. Bernhardt, C. Pasay, J. J. De Voss, J. McCarthy, P. G. Parsons, G. H. Walter, M. T. Smith, H. M. Cooper, S. K. Nilsson, J. Tsanaktsidis, G. P. Savage and C. M. Williams, Validating Eaton's Hypothesis: Cubane as a Benzene Bioisostere, *Angew. Chem., Int. Ed.*, 2016, **55**, 3580–3585.

44 J. Wlochal, R. D. M. Davies and J. Burton, Cubanes in Medicinal Chemistry: Synthesis of Functionalized Building Blocks, *Org. Lett.*, 2014, **16**, 4094–4097.

45 W. A. Palmer and W. Vogler, Cryptostegia grandifolia (Roxb.) R. Br. – rubber vine, in *Biological Control of Weeds in Australia*, ed. M. Julien, R. McFadyen and J. Cullen, CSIRO Publishing, Melbourne, 2012.

46 A. K. Chang and R. G. Duggleby, Herbicide-resistant forms of Arabidopsis thaliana acetohydroxyacid synthase: characterization of the catalytic properties and sensitivity to inhibitors of four defined mutants, *Biochem. J.*, 1998, **333**, 765–777.

47 T. Lonhienne, Y. Cheng, M. D. Garcia, S. H. Hu, Y. S. Low, G. Schenk, C. M. Williams and L. W. Guddat, Structural basis of resistance to herbicides that target acetohydroxyacid synthase, *Nat. Commun.*, 2022, **13**, 3368.

48 J. A. McCourt, S. S. Pang, J. King-Scott, L. W. Guddat and R. G. Duggleby, Herbicide-binding sites revealed in the structure of plant acetohydroxyacid synthase, *Proc. Natl. Acad. Sci. U.S.A.*, 2006, **103**, 569–573.

49 J. G. Wang, P. K. Lee, Y. H. Dong, S. S. Pang, R. G. Duggleby, Z. M. Li and L. W. Guddat, Crystal structures of two novel sulfonylurea herbicides in complex with Arabidopsis thaliana acetohydroxyacid synthase, *FEBS J.*, 2009, **276**, 1282–1290.

50 Y. Cheng, T. Lonhienne, M. D. Garcia, C. M. Williams, G. Schenk and L. W. Guddat, Crystal Structure of the Commercial Herbicide, Amidosulfuron, in Complex with Arabidopsis thaliana Acetohydroxyacid Synthase, *J. Agric. Food Chem.*, 2023, **71**, 5117–5126.

51 I. Belenky, A. Steinmetz, M. Vyazmensky, Z. Barak, K. Tittmann and D. M. Chipman, Many of the functional differences between acetohydroxyacid synthase (AHAS) isozyme I and other AHASs are a result of the rapid formation and breakdown of the covalent acetolactate–thiamin diphosphate adduct in AHAS I, *FEBS J.*, 2012, **279**, 1967–1979.

52 C. Boutin, H. B. Lee, E. T. Peart, P. S. Batchelor and R. J. Maguire, Effects of the sulfonylurea herbicide metsulfuron methyl on growth and reproduction of five wetland and terrestrial plant species, *Environ. Toxicol. Chem.*, 2000, **19**, 2532–2541.